NASA CONTRACTOR REPORT

NASA CR-1170



# RADIATIVE AND CONVECTIVE HEATING DURING ATMOSPHERIC ENTRY

*by W. S. Rigdon, R. B. Dirling, Jr., and M. Thomas*

*Prepared by*
DOUGLAS AIRCRAFT COMPANY
Santa Monica, Calif.
*for Langley Research Center*

NATIONAL AERONAUTICS AND SPACE ADMINISTRATION • WASHINGTON, D. C. • SEPTEMBER 1968

# RADIATIVE AND CONVECTIVE HEATING DURING ATMOSPHERIC ENTRY

By W. S. Rigdon, R. B. Dirling, Jr., and M. Thomas



Prepared under contract No. NAS 1-7757, Item 1, by
DOUGLAS AIRCRAFT COMPANY
Santa Monica, Calif.

for Langley Research Center

NATIONAL AERONAUTICS AND SPACE ADMINISTRATION

For sale by the Clearinghouse for Federal Scientific and Technical Information
Springfield, Virginia 22151 – CFSTI price $3.00

CONTENTS

# RADIATIVE AND CONVECTIVE HEATING DURING ATMOSPHERIC ENTRY

By
W. S. Rigdon, R. B. Dirling, Jr., and M. Thomas
Missile and Space Systems Division
Douglas Aircraft Company
Santa Monica, California

## SUMMARY

The first solutions for radiation-convection coupled stagnation-point heat transfer retaining complete spectral detail of the radiative transfer have been generated for a single entry condition both with and without mass injection. The problems associated with obtaining massive blowing solutions with radiation have been generated for a single entry condition both with and without mass injection. The problems associated with obtaining massive blowing solutions with radiation have been identified and solution procedures developed. The effect of radiative boundary conditions at the wall has been investigated by obtaining solutions for transparent, black, and totally reflecting walls.

The detailed spectral solutions reveal that the originally proposed approximate relation for the divergence of the radiative flux is not suitable for accurate real-gas radiative-convective coupling analyses. Therefore, the radiative transfer processes have been investigated and the theoretical basis for a new approximate formulation for the divergence of the radiative flux has been established such as to account for the dominant real-gas radiative transfer effects.

## INTRODUCTION

For atmospheric entry velocities above escape speed thermal radiation significantly alters the flow field about blunt entry bodies. The predominant effect of the radiance of the hot gas cap is the introduction of enthalpy gradients in the outer shock layer. Thus, when radiative transfer is important the flow field can not be separated into the usual isoenergetic inviscid outer shock layer and a non-adiabatic viscous boundary layer.

This effect has been treated by others using either the gray gas approximation (Reference 1) or polynomial expressions for the velocity and concentration profiles and numerical integration over frequency of radiation (Reference 2). It is now well known that use of the gray gas approximation in radiative transfer calculations for high-temperature air results in serious error. Also the difficulties associated with integrating over frequency while also integrating the conservation equations are obvious (Hoshizaki and Wilson were limited to about 20 frequency points).

As a result of these difficulties many approximate techniques have been developed to solve radiative gasdynamic problems (References 3, 4, 5). In general the accuracy of the various solutions is unknown since no flight experiments have been made above 36,000 fps (NASA's Project FIRE) where coupling is rather weak. In lieu of experimental data for shock layer temperatures of around 15,000°K and large physical size more exact calculations retaining complete spectral detail and as few flow field approximations as possible are required.

The purpose of the present study is twofold. First, solutions for the radiation-convection coupled flow field are to be generated retaining complete spectral detail of the radiant energy transport for selected entry conditions. Secondly, an approximate relation for the divergence of the radiative flux, of such a form as to simplify the analysis of the radiative transfer, is to be obtained.

## NOMENCLATURE

| | |
|---|---|
| $A$ | Defined by Equation (B-2) |
| $A'$ | $(2\pi\ m/h^2)^{3/2}$ |
| Bu | Reference optical depth (Bouguer number) |
| $B_\omega^o$ | Spectral intensity of black body |
| $b$ | Line half-width |
| $C_p$ | Specific heat |
| $c$ | Velocity of light |
| $e$ | Electron charge |
| $\vec{F}$ | Radiative flux vector |
| $f$ | Oscillator strength |
| $g_o, g_\ell$ | Degeneracies of ground and $\ell$th state |
| $h$ | Planck constant; also, altitude |
| $I$ | Intensity of radiation |
| $I_\ell$ | Energy above ground state |
| $K$ | Total thermal conductivity; also proportionality constant (Appendix C) |
| $k$ | Boltzmann constant |
| $k_\omega$ | Linear spectral absorption coefficient |
| $\bar{k}_P$ | Planck mean absorption coefficient |
| $m$ | Electron mass; also degree of ionization |
| $N$ | Species concentration (subscript "e", for electron) |
| $n$ | Principle quantum number |
| $p$ | Pressure |
| $q_r$ | Radiative heat transfer rate |
| $R_N$ | Nose radius |
| $r$ | Radial distance from axis of symmetry |
| $s$ | Line of sight path length |
| $T$ | Temperature |

| | |
|---|---|
| $u$ | Velocity parallel to body |
| $v$ | Velocity normal to body |
| $x$ | Distance parallel to body |
| $y$ | Distance normal to body |
| $\gamma_e$ | Effective line half width |
| $\theta$ | Angle between y unit vector and line of sight path; also hc/kT |
| $\lambda_R$ | Rosseland thermal conductivity |
| $\delta$ | Shock layer thickness |
| $\mu$ | Viscosity |
| $\rho$ | Density |
| $\sigma$ | Stefan-Boltzmann constant |
| $\tau$ | Optical depth |
| $\omega$ | Wave number |

Subscripts

| | |
|---|---|
| c | Critical value; or Continuum |
| i | For $i^{th}$ line |
| L | Line |
| o | Total |
| P | Planck |
| R | Rosseland |
| s | Value immediately downstream of shock |
| w | Wall |
| $\omega$ | Spectral |
| $\infty$ | Free stream |
| 1 | Derived from first term in Equation (A-7) |
| 2 | Derived from second term in Equation (A-7) |

Superscripts

| | |
|---|---|
| + | In positive y-direction; toward shock |
| - | In negative y-direction; toward wall |
| o | Black body |
| ' | With subscript 'P' -- "Planck-like" value, see Equation (A-22) |

## RADIATIVE AND TRANSPORT PROPERTIES OF AIR

The spectral linear absorption coefficient is of critical importance for accurate calculation of the radiative heat transfer to entry vehicles. Since considerable disagreement over the values of the absorption coefficient for air exists in the literature, these quantities were recalculated for this study. A complete description of the spectral absorption coefficient was made including band radiation, photodissociation, photoionization, photodetachment, atomic lines, and brehmsstrahlung. Atomic lines belonging to multiplets were grouped together, since for the conditions of interest the spacing between lines of a particular multiplet was usually of the same order as the line half-widths. This assumption is not critical to the calculation procedure used and was adopted only after transfer calculations showed that line-merging swamps any details of a multiplet in typical shock layers. The f-numbers for the UV lines were taken from NBS (Reference 6) and for the visible lines from Griem (Reference 7). In addition, the hydrogenic model of Stewart and Pyatt (Reference 8) was used to define lines close to the photoelectric edges; this model was used down to the first NBS tabulated line, after which, for lower wave numbers, only the lines tabulated for that species were considered. Lines were obtained for N, $N^+$, O, and $O^+$. By trying several different line representations it was found that radiation transfer would be adequately described if the lines were defined at their center frequency, about a half-width away, and about every 50 $cm^{-1}$ out in the wings.

The modified-hydrogenic model of Penner and Thomas (Reference 9) was used to calculate continuum absorption coefficients for air. This method involves the replacement of the complex mixture of ionized air species with two simple hydrogen-like ions of charge $\overline{m} + \frac{1}{2}$ and $\overline{m} - \frac{1}{2}$, where $\overline{m}$ is the mean charge in the plasma. More details concerning the technique can be found in the work of Dirling, et. al. (Reference 5).

The spectral linear absorption coefficient for air was generated at approximately 2000 spectral points for temperatures from 2000°K to 60,000°K and pressures from 0.003 to 300 atmospheres. The values used for the present

study were scaled according to pressure from the values calculated at 1 atmosphere. Figure 1 shows the values of $k_\omega$ at T = 15,000°K and P = 1 atm.

The transport properties used in this study were calculated by the method described in Reference 10 at the actual stagnation pressure (0.66 atmospheres). Equilibrium concentrations of 18 air species were used and the effects of charge exchange encounters were considered. The viscosity and equilibrium thermal conductivity were calculated to the second-order including the effects of thermal diffusion.

## THE CONSERVATION EQUATIONS

For steady-state, axisymmetric flow, the thin shock layer equations are as follows:

Continuity

$$\frac{\partial(\rho r u)}{\partial x} + \frac{\partial(\rho r v)}{\partial y} = 0 \tag{1}$$

Momentum

$$\rho u \frac{\partial u}{\partial x} + \rho v \frac{\partial u}{\partial y} = - \frac{\partial p}{\partial x} + \frac{1}{r} \frac{\partial}{\partial y} \left( r \mu \frac{\partial u}{\partial y} \right) \tag{2}$$

$$\frac{\partial p}{\partial y} = 0 \tag{3}$$

Energy

$$\rho v C_p \frac{\partial T}{\partial y} = u \frac{\partial p}{\partial x} + \mu \left( \frac{\partial u}{\partial y} \right)^2 + \frac{1}{r} \frac{\partial}{\partial y} \left( r K \frac{\partial T}{\partial y} \right) - \nabla \cdot \vec{F} \tag{4}$$

where $\vec{F}$ is the radiation flux vector.

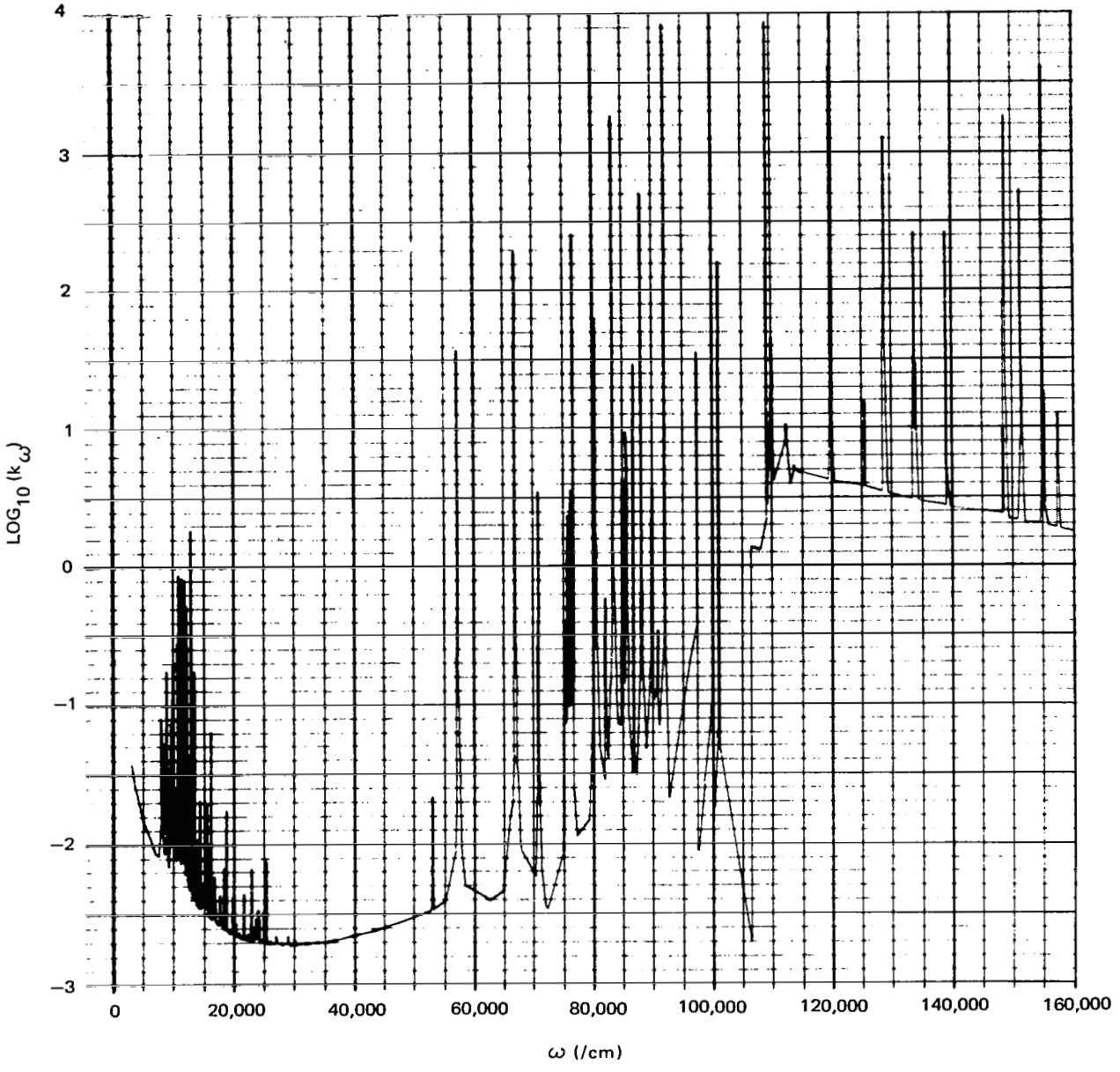


Figure 1. The Spectral Linear Absorption Coefficient of Air for P = 1 atm and T = 15,000°K

At the stagnation point, a similarity transformation is not required to reduce these equations to ordinary differential equations. Applying the conditions at the stagnation point to the above set of equations yields the following:

Momentum and Continuity

$$\frac{d}{dy}\left[\mu\frac{d}{dy}\left(\frac{1}{\rho}\frac{d(\rho v)}{dy}\right)\right] - \rho v\frac{d}{dy}\left(\frac{1}{\rho}\frac{d(\rho v)}{dy}\right) - \left[2\rho_s\left(\frac{du_s}{dx}\right)^2 - \frac{\rho}{2}\left(\frac{1}{\rho}\frac{d(\rho v)}{dy}\right)^2\right] = 0 \qquad (5)$$

Energy

$$\rho v C_p\frac{dT}{dy} = \frac{d}{dy}\left(K\frac{dT}{dy}\right) - (\nabla\cdot\vec{F})_y \qquad (6)$$

Here $(\nabla\cdot\vec{F})_y$ is the divergence of the radiation flux normal to the body surface.† The normal boundary conditions to be used in the study are

| at the wall | at the shock |
|---|---|
| $\rho v = 0$ | $\rho v = \rho_\infty v_\infty$ |
| $\frac{1}{\rho}\frac{\partial(\rho v)}{\partial y} = 0$ | $\frac{1}{\rho}\frac{\partial(\rho v)}{\partial y} = -2\frac{du_s}{dx}$ |
| $T = T_w$ | $T = T_s$ |

For cases where mass transfer is to be considered, $\rho v$ at the wall is altered appropriately.

†Throughout the remainder of this report the symbols $\nabla\cdot\vec{F}$ and $\frac{dF}{dy}$ will be used interchangeably to denote the divergence of the radiation flux normal to the body surface, $(\nabla\cdot\vec{F})_y$.

## DETAILED SOLUTIONS

The radiative transfer through a non-scattering medium is described by the Lambert-Bouguer equation

$$\frac{dI_\omega}{ds} = k_\omega \left[ B^o_\omega - I_\omega \right] \tag{7}$$

The positive and negative y-components of the flux are given by the following equations

$$F^+ \ (y) = -2\pi \int_{\theta = 0}^{\pi/2} \int_0^\infty I_\omega(y, \theta) \cos\theta \, d\omega \, d(\cos\theta) \tag{8a}$$

$$F^- \ (y) = -2\pi \int_{\theta = \pi/2}^{\pi} \int_0^\infty I_\omega(y, \theta) \cos\theta \, d\omega \, d(\cos\theta) \tag{8b}$$

Similarly

$$\frac{dF^+}{dy} = -2\pi \int_{\theta = 0}^{\pi/2} \int_0^\infty \frac{dI_\omega}{ds} d\omega \, d(\cos\theta) \tag{9a}$$

$$\frac{dF^-}{dy} = -2\pi \int_{\theta = \pi/2}^{\pi} \int_0^\infty \frac{dI_\omega}{ds} d\omega \, d(\cos\theta) \tag{9b}$$

and

$$\frac{dF}{dy} = \frac{dF^+}{dy} + \frac{dF^-}{dy}$$

The radiative-transfer code (STER, HO4O) solves Equation (7) using second-order Runge-Kutta for the most part. When the intensity at any frequency becomes close to the black-body value, the asymptotic form of Equation (7)

$$I_\omega \approx B^o_\omega - \frac{1}{k_\omega} \frac{\partial B^o_\omega}{\partial s}$$

is used. The use of this asymptotic expression for the intensity allows very large integration intervals to be used, typically about 1/100th of the shock-layer thickness, rather than intervals of the order of $1/k_\omega$ required for integration stability. The intensity for eight different slant directions through the layer is found by simultaneous integration along each path; fluxes are then determined by Gaussian quadrature.

The radiative flux emergent from a shock layer can be calculated retaining the full spectral detail and integration accuracy in about two minutes on the Univac 1108 computer (about 5 minutes on the IBM 7094). It is apparent that such detailed calculations would be very expensive if coupled to an iterative solution of a high-temperature flow-field problem.

The Radiative Transfer Computer Program (STER) was modified to compute the divergence of the flux using numerical differentiation and an infinite slab geometry. This program permits the evaluation of the net emission from an elemental volume of gas provided the temperature profile is known. In this investigation an iterative technique is employed to obtain flow-field solutions with detailed spectral evaluation of the net radiant emission (divergence of the radiative flux). Tabular values of the net emission as a function of $\rho v$ are used in the solution of the conservation equations to obtain solution curves for the temperature. New values for the flux and net emission are then computed using the modified radiative-transfer code (STER) considering approximately 1000 wave number points. Iteration is continued until the $\nabla \cdot \vec{F}$ profiles converge.

Figures 2 and 3 present the flow field and $\nabla \cdot \vec{F}$ profiles obtained from the detailed solution of the conservation equations with no mass injection for the indicated entry conditions. For this case the $\nabla \cdot \vec{F}$ was evaluated under the assumption that the wall is transparent. That is, the radiation boundary conditions at the wall are

$$I_\omega(0, \theta) = 0 \quad \text{for all } \omega \quad \text{and} \quad 0 \le \theta \le \pi/2$$

or

$$F_\omega^+(0) = 0 \qquad \text{for all } \omega$$

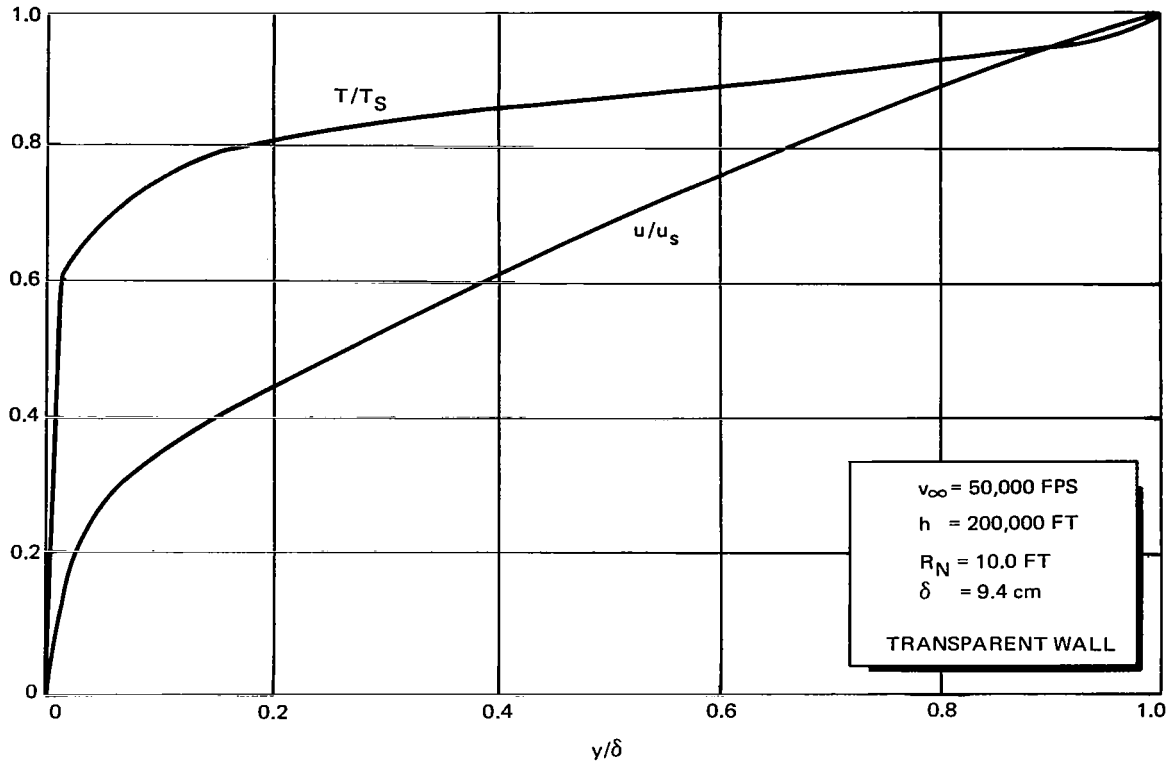


Figure 2. Flow Field with Radiative Coupling Without Blowing

The convective and radiative heat fluxes at the wall are 600 watts/sq cm and 5296 watts/sq cm, respectively. Detailed spectral solutions for this case were also generated for both black and perfectly reflecting walls. The radiation boundary conditions at the wall for these two cases are as follows:

black wall

$$I_\omega(0, \theta) = B^o_\omega(0) \quad \text{for all } \omega \quad \text{and} \quad 0 \le \theta \le \pi/2$$

$$F^+_\omega(0) = \pi B^o_\omega(0) \quad \text{for all } \omega$$

reflecting wall

$$I_\omega(0, \theta) = I_\omega(0, \pi - \theta) \quad \text{for all } \omega \quad \text{and } 0 \le \theta \le \pi/2$$

$$F^+_\omega(0) = -F^-_\omega(0) \quad \text{for all } \omega$$

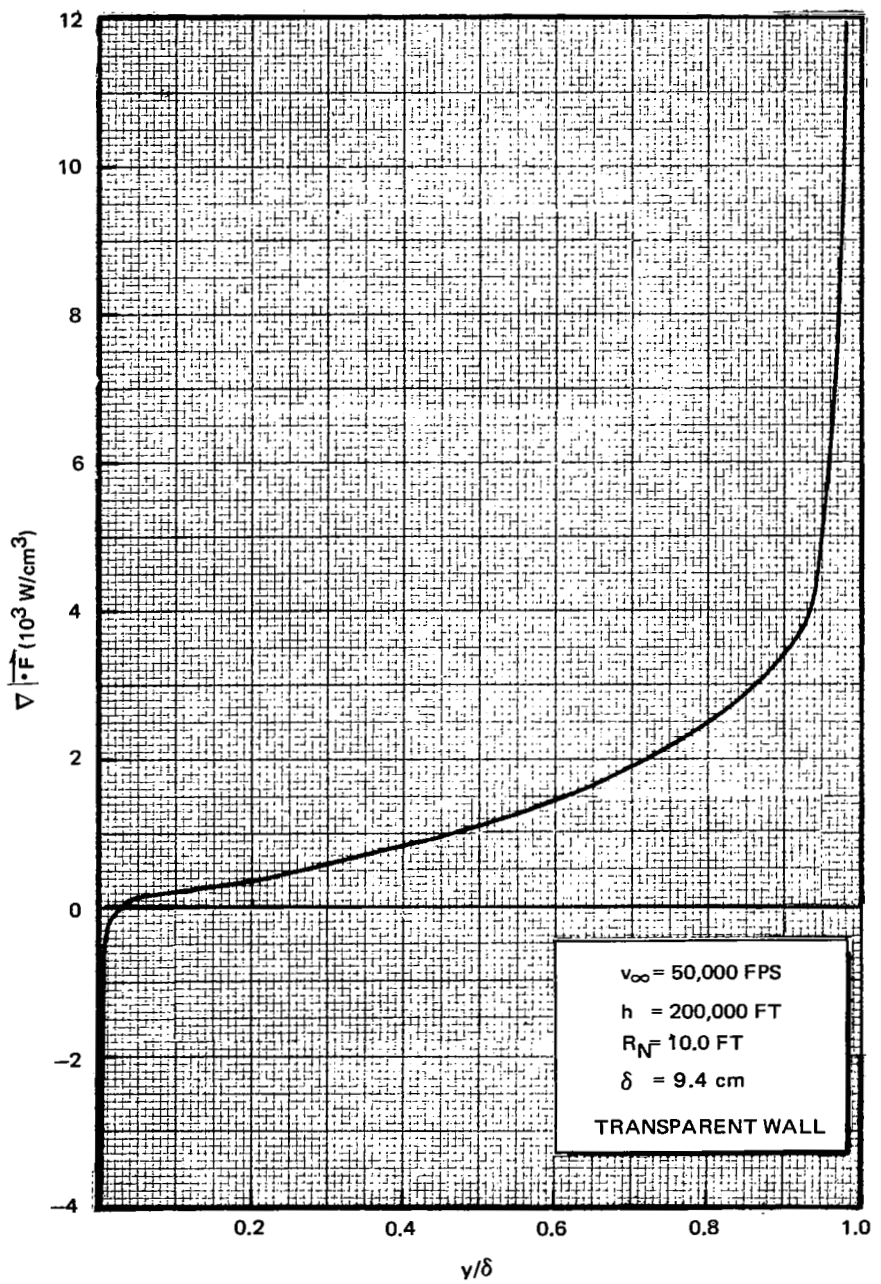


Figure 3. Net Radiant Energy Emission for Shock Layer with no Blowing

Calculation of the net radiant emission assuming a totally black wall results in values identical (within the accuracy of the calculations) to those obtained for transparent walls. For a reflecting wall the convective heat flux is increased to 980 watts/sq cm. Figure 4 presents a comparison of the transparent and reflecting wall temperature profiles.

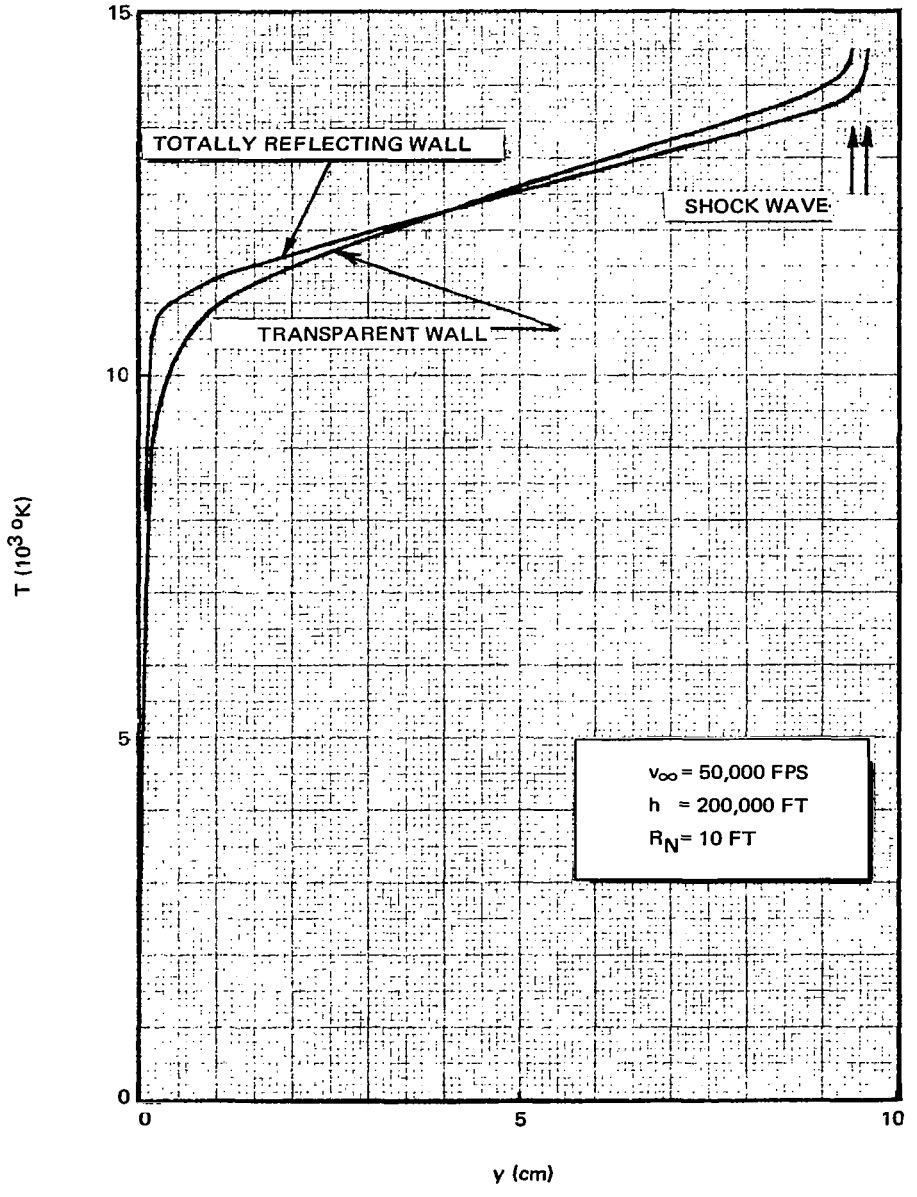


**Figure 4. Temperature Profiles Showing the Effect of Wall Reflectivity with no Blowing**

Solution of the conservation equations with strong blowing is especially important at high entry velocities because the radiative heat transfer will induce massive ablation of the vehicle surface. Thus, it is imperative to understand the effects of large blowing rates on the shock-layer flow-field structure and the attendant changes in radiative and convective heat-transfer rates. Ideally, of course, one would like to carry out this investigation using radiative and transport properties for the blown gas mixture which correspond to the complex molecules present in the ablation products of most heat-shield materials. The present investigation is limited to a blown gas whose properties are identical to those of air. While some previous investigations (References 2 and 11) have indicated that radiative absorption by complex molecules has little effect on the heat-transfer rates at the wall, it should be pointed out that the entry conditions and blowing rates used in these studies were such that the blown layer was relatively thin.

The entry conditions and blowing rate used in the present study correspond to what would be a classical shear-layer solution if radiative coupling were neglected. This is illustrated in Figure 5 which shows the temperature and tangential velocity profiles obtained by integrating the conservation equations with $\nabla \cdot \vec{F}$ set to zero. The region from the wall to about y = 0.9 cm has the properties of constant shear and temperature and the region of maximum shear is displaced from the wall by the same amount. It is evident from Figure 6, which presents the net radiative emission from this shock layer, that the classical shear-layer solution with zero convective heat transfer at the wall is not possible when radiation is an important mode of energy transport to the shock layer. That is, if the $\nabla \cdot \vec{F}$ of Figure 6 is integrated from $y = 0$ to $y = \tilde{y}$ where $\tilde{y}$ is a point immediately before the temperature starts to rise rapidly, one finds that

$$q_r(\tilde{y}) - q_r(0) = -1436 \text{ watts/cm}^2$$

Thus 1436 watts/cm$^2$ in radiant energy is absorbed by the constant shear-layer and this would require that the convective heat-transfer rate at the wall be that same value to maintain steady state (neglecting the energy

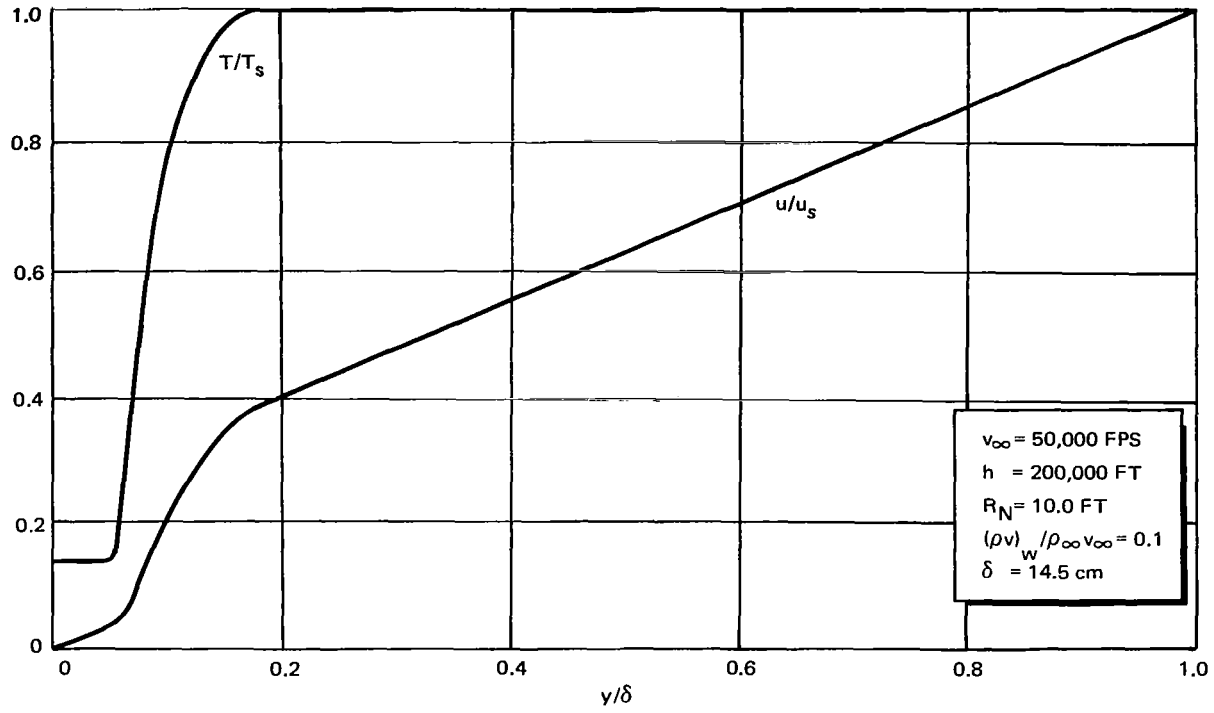


Figure 5. Flow Field with Massive Blowing and no Radiative Coupling

transported in the u direction). In actuality, of course, the convective heat-transfer rate is somewhere in between the two extremes of zero and 1436 watts/cm$^2$.

Before presenting the results obtained for the detailed solution of the radiative coupled shock layer with massive blowing, a discussion of the problems encountered and the resulting techniques developed will be presented. Two major problem areas were discovered: (1) integration of the energy and momentum equation in regions of positive ρv, and (2) input of the calculated $\nabla \cdot \vec{F}$ profile for the next integration of the conservation equations.

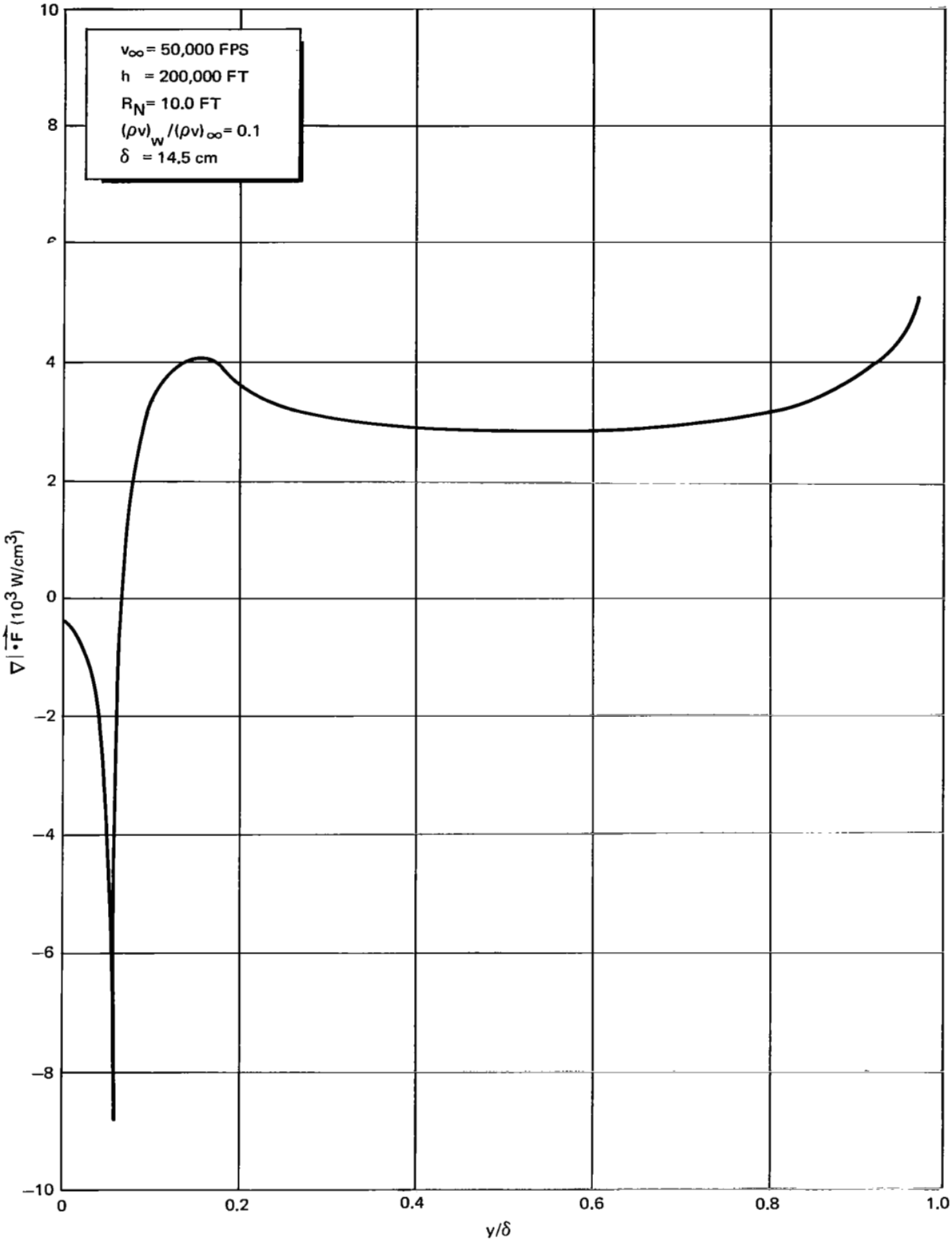


Figure 6. Net Radiative Energy Emission Computed for Massive Blowing Temperature Profile with no Radiative Coupling

Integral solutions of both the momentum and energy equations can be easily obtained. For instance, the solution of the energy equation is

$$Q(y) = \exp\left[\int_0^y \rho v \frac{C_p}{K}\, d\xi\right]\left\{\int_0^y \frac{\nabla \cdot \vec{F}(\xi)\, d\xi}{\exp\left[\int_0^\xi \rho v \frac{C_p}{K}\, d\zeta\right]} + Q(0)\right\}$$

where

$$Q = K\frac{dT}{dy}$$

This equation shows that small errors in the choice of $Q(0)$ cause the difference between the calculated and correct $Q(y)$ values to grow exponentially in the region of positive $\rho v$. Since $\rho v C_p/K$ is of the order of 1 to 10 for the case considered here the error grows very fast. The situation is exactly the same when the momentum equation is considered. In general the requirement that both of these equations be integrated simultaneously means that varying the values of the convective heat-transfer rate and the shear stress at the wall is not a practical way to satisfy boundary conditions imposed at the shock.

In order to overcome this difficulty one might immediately propose that the numerical integration be started at $\rho v = 0$ (i. e., away from the wall) and proceed in both directions. While this procedure eliminates the numerical integration instability in the blown gas region it requires that four eigenvalues be iterated upon (T, u, dT/dy and the shear stress -- all evaluated at $\rho v = 0$) and that the boundary conditions on T and u be matched at both the wall and the shock. The addition of two more eigenvalues quadruples the complexity of the iteration procedure required since there are now sixteen derivatives of the end values instead of four as when integration is started at the wall. A second problem area was identified when this integration method was attempted.

Tabular values of $\nabla \cdot \vec{F}$ are input in the solution of the energy equation as a function of $\rho v$. This is necessary to insure the inclusion of the extremely large values of $\nabla \cdot \vec{F}$ close to the shock front. When integration is started at $\rho v$ equal to zero and continued toward the wall it is doubly important that $\rho v$ be the independent variable in order to include the high reabsorption area near the wall. However, since the derivative of $\rho v$ is proportional to the tangential velocity which is zero at the wall, the wall reabsorption spike occurs in a region of almost constant $\rho v$. If the numerical integration procedure is started at the wall, u is set identically to zero at the wall and $\rho v$ varies properly with y so that no errors are introduced in the width of the reabsorption spike due to transformation from $\rho v$ to y coordinates. However, when integration is started at $\rho v$ equal to zero, the value of u at the wall is a boundary condition which must be matched to within some accuracy criteria. That is, the tangential velocity at the wall has some small value not equal to zero. This small change in the slope of $\rho v$ at the wall affects the absolute width (on the y scale) of the reabsorption spike significantly. In fact it appears that the accuracy criteria on the u velocity at the wall must be at least

$$u(\rho v = \rho v_w) \leq 0.005\, u(\rho v = \rho v_s)$$

The integration difficulties associated with this problem are overcome by switching from $\rho v$-values to u-values as the independent variable used to evaluate $\nabla \cdot \vec{F}$ near the wall.

Figure 7 shows the temperature and tangential velocity profiles obtained for the detailed solution of the massive blowing case. Figure 8 presents the associated $\nabla \cdot \vec{F}$ profile.

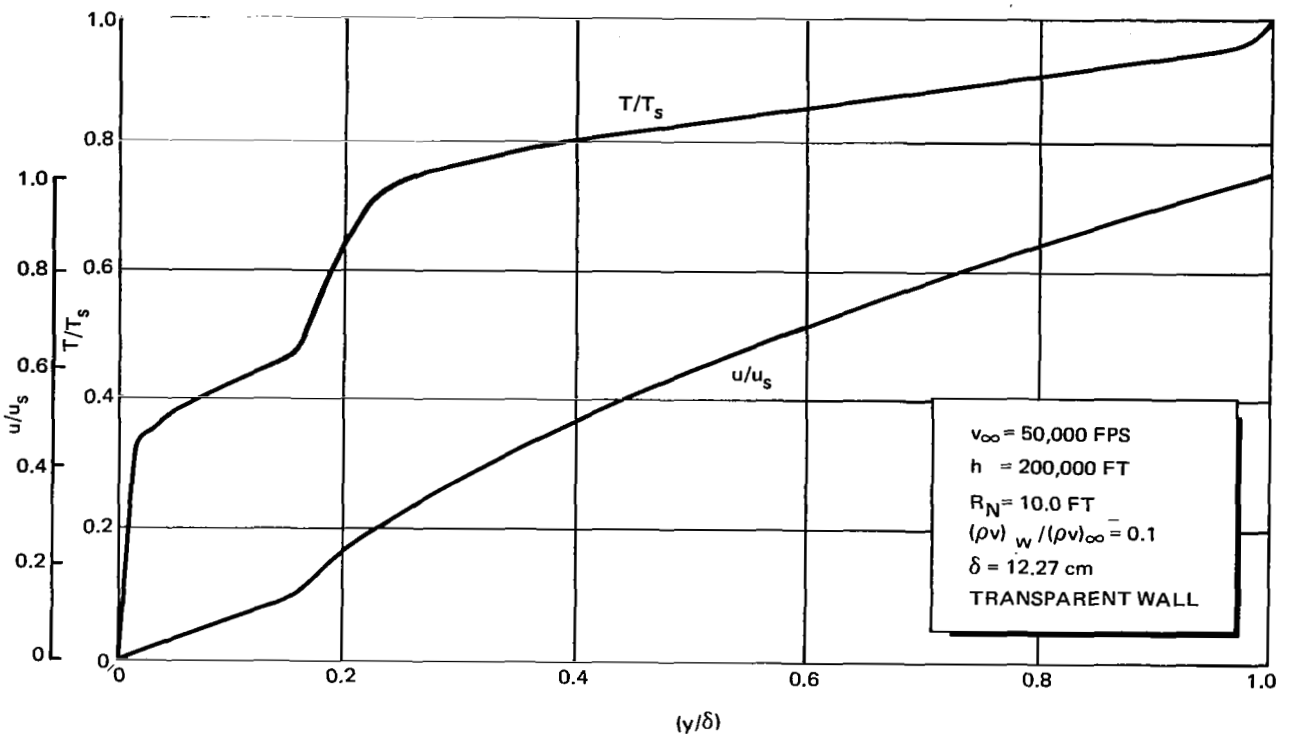


Figure 7. Flow Field with Massive Blowing and Radiative Coupling

The entire region of blown gas has a substantial net absorption of radiant energy indicating that the conversion of radiant to convective energy is very important for strong blowing. It appears then that if the blown gas were composed of ablation products including complex molecules which have substantially larger absorption coefficients than air, the conversion of radiative to convective energy would be greatly enhanced. The convective and radiative heat fluxes at the wall for this case are 135 watts/sq cm and 4322 watts/sq cm, respectively.

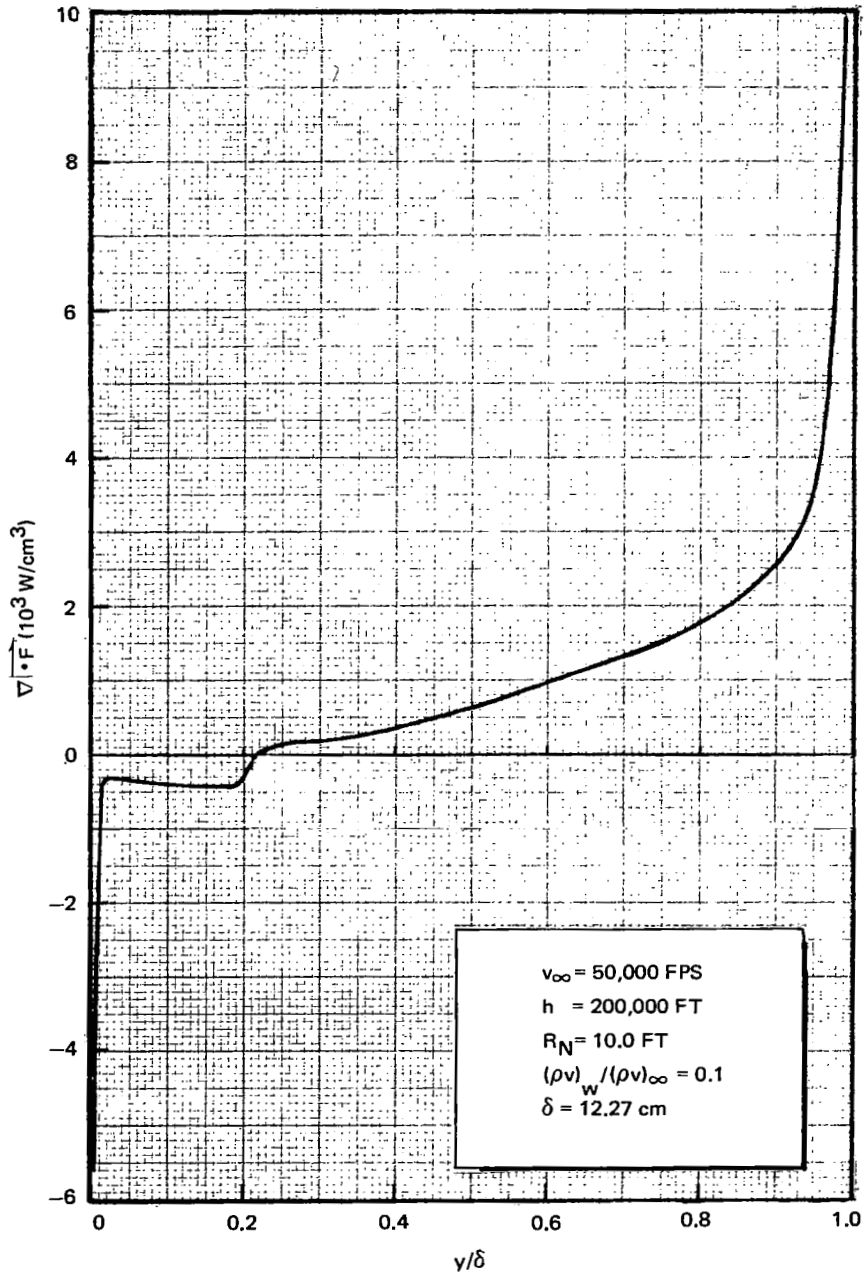


Figure 8. Net Radiant Energy Emission for Shock Layer with Massive Blowing and Radiative Coupling

Table 1 presents a summary of the heat transfer rates obtained for the detailed spectral shock-layer solutions. Also presented are the heat flux values for the corresponding uncoupled solutions. The uncoupled convective heat transfer rates are obtained from solutions of the conservation equations with $\nabla \cdot \vec{F}$ set equal to zero, while the radiative fluxes are obtained by integrating Equation (7) for the resulting temperature profiles. Comparison of the coupled and uncoupled fluxes reveals that the entry condition considered in this study corresponds to a condition of strong coupling.

TABLE 1

SUMMARY OF CASES STUDIED

$v_\infty$ = 50,000 ft/sec h = 200,000 ft $T_w$ = 2000° K

| $R_N$ (ft) | Wall Boundary Condition | $\frac{(\rho v)_w}{\rho_\infty v_\infty}$ | $q_c$ | $q_r$ | $q_t$ |
|---|---|---|---|---|---|
| 10.0 | Transparent | 0 | 600 (409) | 5296 (21,521) | 5896 |
| 10.0 | Transparent | 0.1 | 135 ( 0 ) | 4322 (11,937) | 4457 |
| 10.0 | Totally Reflecting | 0 | 980 | -- | 980 |
| 10.0 | Black | 0 | 600 | 5296 | 5896 |

Notes: 1. Heat transfer rates in watts/$cm^2$.
2. Numbers in parenthesis refer to uncoupled heat transfer rates.

## AN APPROXIMATION FOR $\nabla \cdot \vec{F}$

An approximate expression for the divergence of the radiant energy flux is sought for two reasons. First, calculations of coupled radiation-flow fields are often prohibitively time-consuming using currently available computers. Second, the approximation of exact integral relations for radiation transport by simpler expressions helps isolate the important mechanisms of radiant transport and, hence, furthers basic understanding of the phenomena. For the current study, an approximation for $\nabla \cdot \vec{F}$ is required that will be sufficiently accurate to make parametric studies possible, with only a minimum number of detailed spectral calculations of the radiant energy transport.

The model originally proposed to be used to approximate $\nabla \cdot \vec{F}$ is based upon interpolation between the limits of a transparent and opaque gas. The expression developed was

$$\nabla \cdot \vec{F} = \frac{4 Bu_P \bar{k}_P \sigma T^4}{Bu_P + \tau_{P_i}} - \frac{d}{dy}\left(\frac{\tau^* \lambda_R}{Bu_R + \tau^*} \frac{dT}{dy}\right) \tag{10}$$

where

$\tau_{P_i}$ = Planck optical depth to nearest wall

$$\tau^* = \tau_{R_i}\left[\frac{2}{\tau_{P_o} + \tau_{R_o}} \frac{\tau_{R_o}}{\tau_{P_o}} \left|\frac{d(T/T_s)}{d\tau_R}\right|\right]^{-1}$$

$\tau_{R_i}$ = Rosseland optical depth to nearest wall,

and a subscript "o" refers to total layer thickness.

Previous calculations have shown that Equation (10) gives an accurate representation of radiative-conduction coupling for the special cases of a gray gas

or a two-step simple non-gray model (References 5 and 12). The approximation was also used to obtain coupled convective-radiative flow fields at the stagnation point of planetary-return entry vehicles (Reference 5) and it was discovered that the effects of radiative cooling were more important than had previously been expected or calculated. Much more accurate values of the spectral absorption coefficients are now available than those used for that study. Therefore, before applying the approximate formula for a parametric study, a more sophisticated analysis was warranted.

The previous study of coupling during superorbital reentry showed that the dominant mode of radiative energy transport was atomic-line radiation. Thus, typical shock layers become neither optically thin nor optically thick in the sense of Equation (10), because of the extreme variations of atomic-line absorption coefficients through the spectrum. In fact the optically-thin region of the spectrum is confined to a gas layer several microns thick near the shock, while the shock layer is never optically thick at all because of weak absorption in the wings of lines. Equation (10) is therefore not useful for typical shock layers and a more applicable formula was sought.

Atomic-Line Transfer

Because of the strong line structure of high-temperature air, Equation (10) must be replaced by terms adequate to describe line transfer. When lines are weak, the first term in Equation (10) is still valid, since the weak-line model gives

$$\nabla \cdot \vec{F}^{+} = 2\bar{k}_P \sigma T^4 \tag{11}$$

For the case of strong lines, the following can be derived (Appendix A):

$$\nabla \cdot \vec{F}^{+} = \frac{16\sigma}{3} \frac{dT}{dy} T^3 \sqrt{\tau_L} + 2\bar{k}'_P \frac{\sigma T^4}{\sqrt{\tau'_P}} \tag{12}$$

We now postulate a form for $\nabla \cdot \vec{F}^{+}$ that reduces to these two limits of large and small optical depth -- the same technique that led to the good correlations of grey-gas radiative transfer (Reference 12)

$$\nabla \cdot \vec{F}^{+}_{\text{lines}} = 2\bar{k}_P \sigma T^4 \left( \frac{Bu_P}{Bu_P + \tau_P} \right)^{1/2} + \frac{16\sigma}{3} \frac{dT}{dy} T^3 \frac{\tau_L}{(Bu_L + \tau_L)^{1/2}} \quad (13)$$

where the first term is a "Planck-like" expression and the second term is a "Rosseland-like" expression. Note that Equation (13) reduces to Equation (12) for large optical depth if

$$\frac{\bar{k}'_P}{\sqrt{\tau'_P}} = \frac{\bar{k}_P}{\sqrt{\tau_P}} \, Bu_P^{1/2} \quad (14)$$

Thus $Bu_P$ acts as a conversion factor to change the normal Planck mean absorption coefficients to the primed values (defined by Equation (A-22) in Appendix A). Thus we have imposed a double role on $Bu_P$ in this model -- a conversion factor and a characteristic optical depth. Such an imposition is justified if Equation (13) correlates results found by detailed spectral calculations.

This result is not presented as rigorously derived, but rather a result of a heuristic argument of a type proven in previous studies to be valuable. The divergence depends upon two parameters, $Bu_P$ and $Bu_L$, which represent characteristic optical depths at which the medium can be treated as optically thin or optically thick. The usefulness of the expression will be determined in its ability to correlate with exact calculations.

Throughout most of the shock layer, line transfer is the dominant mode of radiation. For instance, using the shock-layer temperature profile in Figure 2, detailed spectral calculations of the flux divergence show the domination of lines and the change from thin to thick behavior. Figure 9 shows, as a function of the upper limit of integration, $\int_0^{\omega} \nabla \cdot \vec{F}_{\omega}^{-} \, d\omega$ for

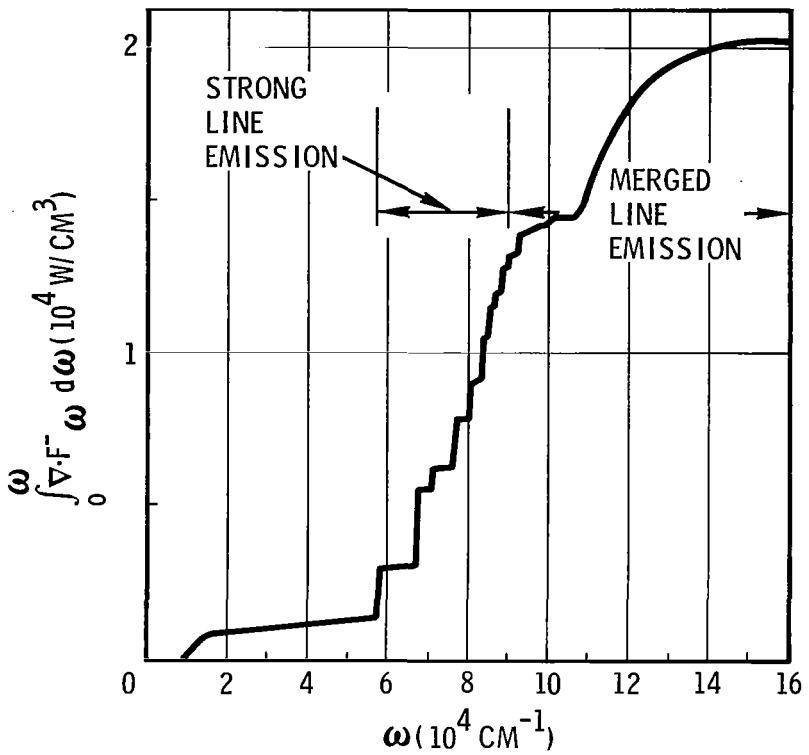


Figure 9. The Integrated $\nabla \cdot F_\omega$ for Shock-Layer Radiation Traveling Toward the Cold Wall, Evaluated 0.04 cm from the Shock

radiation emitted near the shock toward the cold wall. (The value of the integral at $\omega = 160,000\ cm^{-1}$ is essentially the total contribution to $\nabla \cdot \vec{F}^-$ at this shock-layer position; integration to higher wave numbers is unwarranted.) The large step contributions to $\int_0^\omega \nabla \cdot F_\omega^- \, d\omega$ in the region $60,000 > \omega < 80,000\ cm^{-1}$ are caused by line emission; for larger wave numbers, the steps become smaller as line merging becomes significant near the photoelectric edges. For the $F^-$ flux and these optical thicknesses, the "Planck-like" term in Equation (13) dominates and yields the characteristic region of high net emission close to the shock found in the detailed $\nabla \cdot \vec{F}$ calculations. At the other side of the shock layer, the radiation traveling toward the wall has traversed a large optical thickness and the "Rosseland-like" term in Equation (13) should become dominant. Figure 10 shows exact

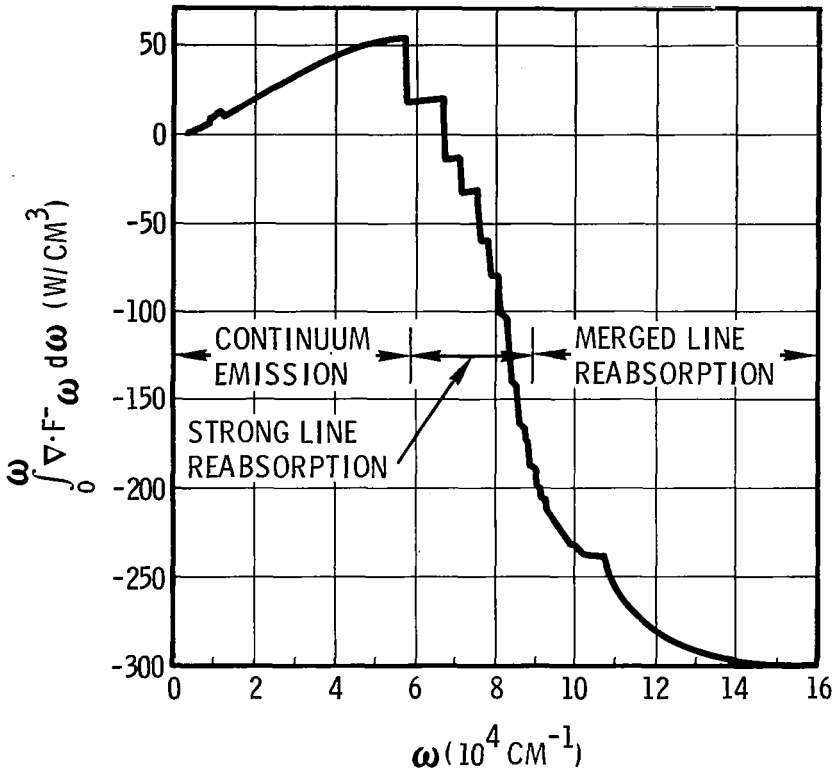


Figure 10. The Integrated $\nabla \cdot F_\omega$ for Shock-Layer Radiation Traveling Toward the Cold Wall, Evaluated 1.18 cm from the Wall

calculations at a position 1.18 cm from the cold wall and the step decreases in intensity associated with line self-reversal is evident.

## Continuum Contribution

Although line transfer is the most important mode of energy transport, continuum contributions are not negligible. For instance, Figure 11 shows the contribution to the integral of $\nabla \cdot \bar{F}_\omega^-$ over wave number for the flux moving toward the cold wall at a position very close to the wall. (The temperature profile is again that of Figure 2). The step decreases in the integral, caused by distinct lines, as shown in Figure 10, have disappeared showing that the UV merged-line and photoionization continuum is now the principle mode of energy absorption.

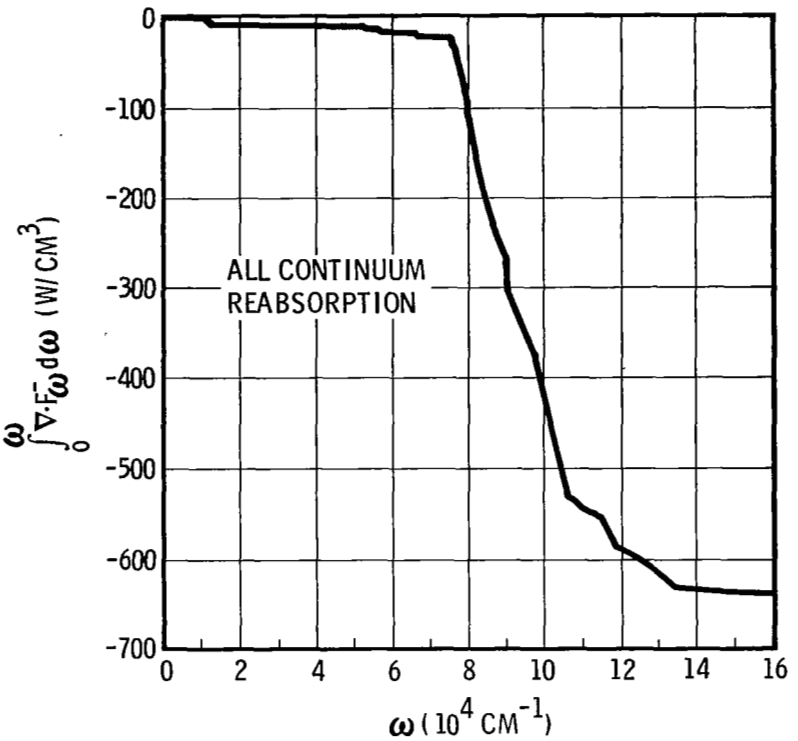


Figure 11. The Integrated $\nabla \cdot F_\omega$ for Shock-Layer Radiation Traveling Toward the Cold Wall, Evaluated 0.11 cm from the Wall

To treat this effect, two models are proposed.

1. Optically thick continuum transfer.
2. Pure absorption by the continuum.

Only the first has been extensively investigated in this study. It appears that the second model will be more useful; this fact was discovered late in the study after a sufficient volume of detailed spectral calculations had been made. The first model is based on a hydrogenic continuum ($k_\omega \propto \omega^{-3}$), and yields (Appendix B)

$$\nabla \cdot \vec{F}^+ = \frac{15}{\pi^4} \sigma T^3 \frac{dT}{dy} \left( \frac{hc\,\omega_c}{kT} + 1 \right)^4 \exp\left( - \frac{hc\,\omega_c}{kT} \right) \qquad (15)$$

Then, a postulated equation, reducing to the correct thick and thin limits, is

$$\nabla \cdot \vec{F}^{+} = \frac{15}{\pi^4} \sigma T^3 \frac{dT}{dy} \left( \frac{hc\,\omega_c}{kT} + 1 \right)^4 \exp\left( - \frac{hc\,\omega_c}{kT} \right) \left( \frac{\tau_c}{Bu_c + \tau_c} \right)^{1/2} \tag{16}$$

where $\tau_c$ is a reference optical depth evaluated at $\omega = 1\ cm^{-1}$ (Appendix B).

These same arguments apply also to the left-moving flux, so that $\nabla \cdot \vec{F}^{-}$ is also given by Equations (13) and (16) with the optical depths measured from the other boundary.

The second model of continuum transfer is one of pure absorption. Assuming a grey, isotropic radiation field with no local emission, then the following relation can be derived (Appendix C).

$$\nabla \cdot \vec{F}^{+} = - \frac{4\pi ck}{\sigma T^3} \exp\left( - \frac{hc\omega_c}{kT} \right) A F^{+} \tag{17}$$

Following our usual procedure, we postulate that the form

$$\nabla \cdot \vec{F}^{+} = - \frac{4\pi ck}{\sigma T^3} \exp\left( - \frac{hc\omega_c}{kT} \right) A F^{+} \left( \frac{\tau_c}{Bu_c + \tau_c} \right)^{1/2} \tag{18}$$

will correlate the divergence of the right-moving flux in the blown-gas layer.

For this study, Equations (13) and (16) are combined to give

$$\nabla \cdot \vec{F}^{+} = 2\bar{k}_P \sigma T^4 \left( \frac{Bu_P}{Bu_P + \tau_P} \right)^{1/2} + \frac{16\sigma}{3} \frac{dT}{dy} T^3 \frac{\tau_L}{(Bu_L + \tau_L)^{1/2}}$$

$$+ \frac{15}{\pi^4} \sigma T^3 \frac{dT}{dy} \left( \frac{hc\,\omega_c}{kT} + 1 \right)^4 \exp\left( - \frac{hc\,\omega_c}{kT} \right) \left( \frac{\tau_c}{Bu_c + \tau_c} \right)^{1/2} \tag{19}$$

and a similar expression is obtained for $\nabla \cdot \vec{F}^-$, with the optical depths measured from the other boundary. We have investigated two different applications of Equation (19) corresponding to dominance of continuum radiation or dominance of line radiation in the reabsorption regions. These correspond to the choice of $\omega_c = 58000\ cm^{-1}$ (associated with the effective continuum created by merged, reversed lines) and $\omega_c = 110,000\ cm^{-1}$ (associated with the photoelectric edges), respectively.

## Comparison of Detailed and Approximate Solutions

The $\nabla \cdot \vec{F}$ profiles computed using both the detailed spectral method and Equation (19) for a temperature profile like that in Figure 2 are shown in Figure 12. The left-moving and right-moving contributions to the detailed and approximate divergences of the flux are shown in Figure 13. The total energy received at the wall and transmitted through the shock were 5029 and 10037 $W/cm^2$, respectively. For the case of line-radiation dominance $Bu_c$ was chosen as $Bu_c = \left(\tau_{co}/\tau_{Lo}\right)Bu_L$ since the continuum term is relatively unimportant. Similarly, for the case of continuum-radiation dominance, $Bu_L = \left(\tau_{Lo}/\tau_{co}\right)Bu_c$. Then $Bu_P$ and either $Bu_c$ or $Bu_L$, depending on whether continuum or line dominance is assumed, are adjusted until $F^-$ and $F^+$ at the boundaries match the detail calculations. For the example presented here, this procedure gave the correlations shown in Figures 12 to 15 for the two cases considered. The matching of $\nabla \cdot \vec{F}$ by the approximate form is seen to be quite good over most of the shock layer. The continuum-dominant model yields a somewhat more accurate fit in the reabsorption region near the cold wall.

Results for the solutions with blowing are shown in Figures 16 and 17. The agreement between the approximate method and detailed spectral calculations is again good over most of the shock layer. However, the approximate calculation shows poor agreement in the blown-gas layer (for distances from the wall less than 3 cm). The magnitude of total energy deposition in the layer is about correct, but the approximate method deposits it all in the region of strong temperature change at the boundary between the blowing gases and the outer shock layer. The detailed calculations show a more even deposition through the blown-gas layer.

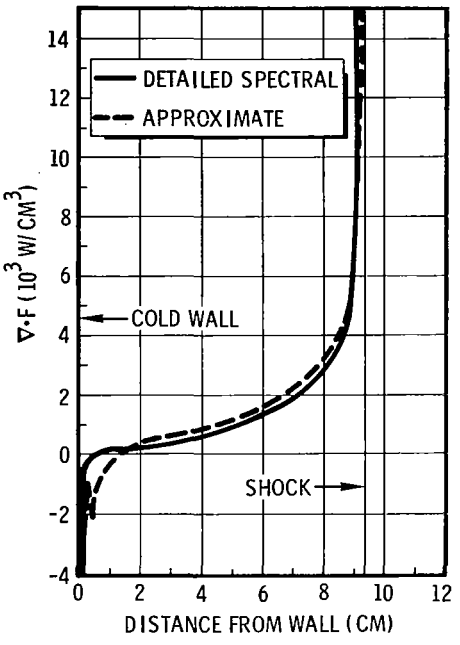


Figure 12. Divergence of Shock-Layer Radiation Compared to Approximation Using Line-Dominant Reabsorption Model. $Bu_{\bar{P}} = 0.00004$, $Bu_L = 0.008$

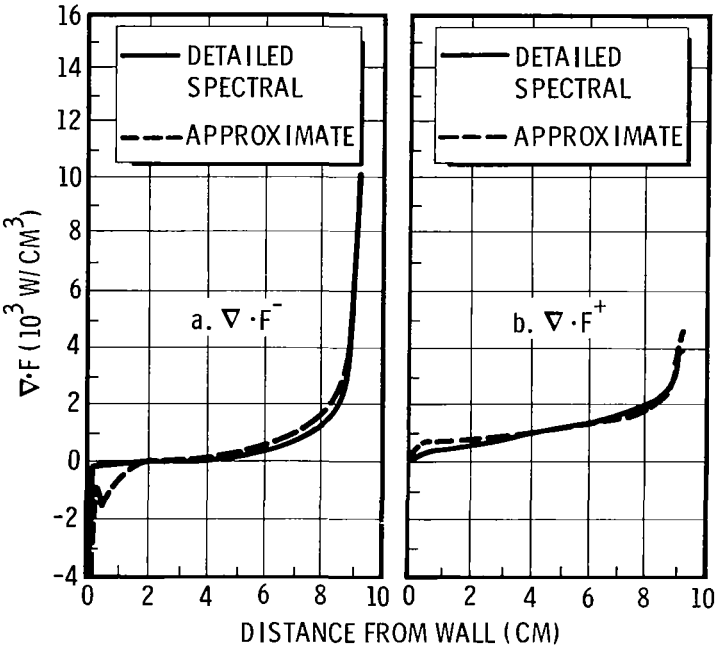


Figure 13. The Divergence of Shock-Layer Radiation Split into its Left-Moving and Right-Moving Components, Compared to Approximation Using Line-Dominant Reabsorption Model. $Bu_P = 0.00004$, $Bu_L = 0.008$

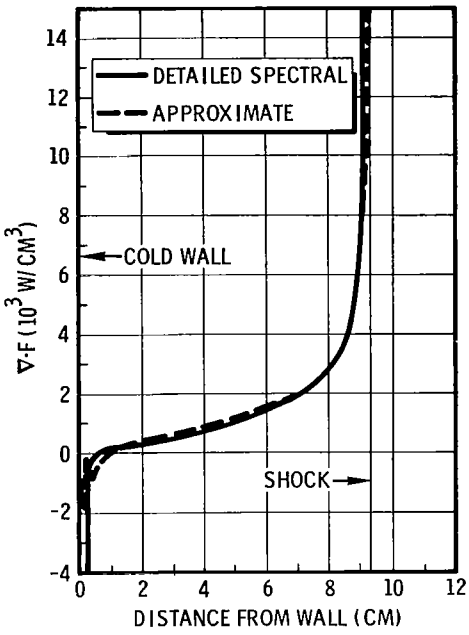


Figure 14. Divergence of Shock-Layer Radiation Compared to Approximation Using Continuum-Dominant Reabsorption Model. $Bu_P = 0.000025$, $Bu_L = 0.006$

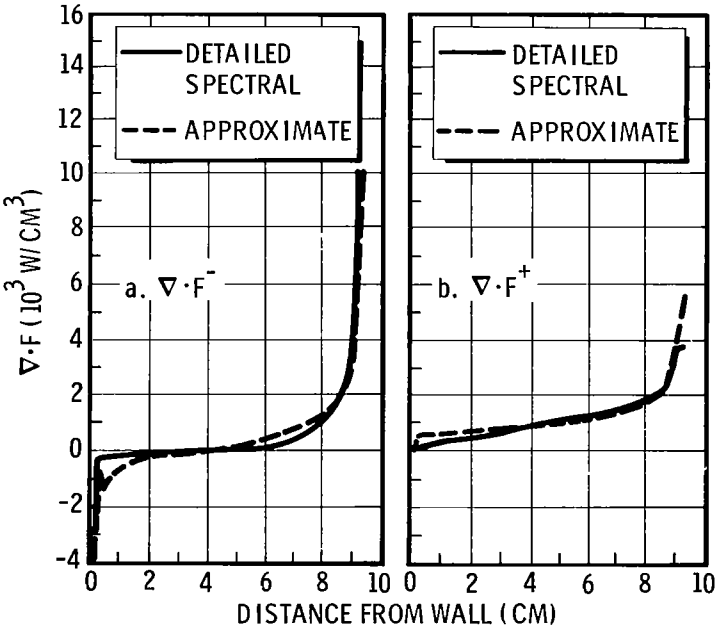


Figure 15. The Divergence of Shock-Layer Radiation Split into its Left-Moving and Right-Moving Components, Compared to Approximation using Continuum-Dominant Reabsorption Model. $Bu_P = 0.000025$, $Bu_L = 0.006$

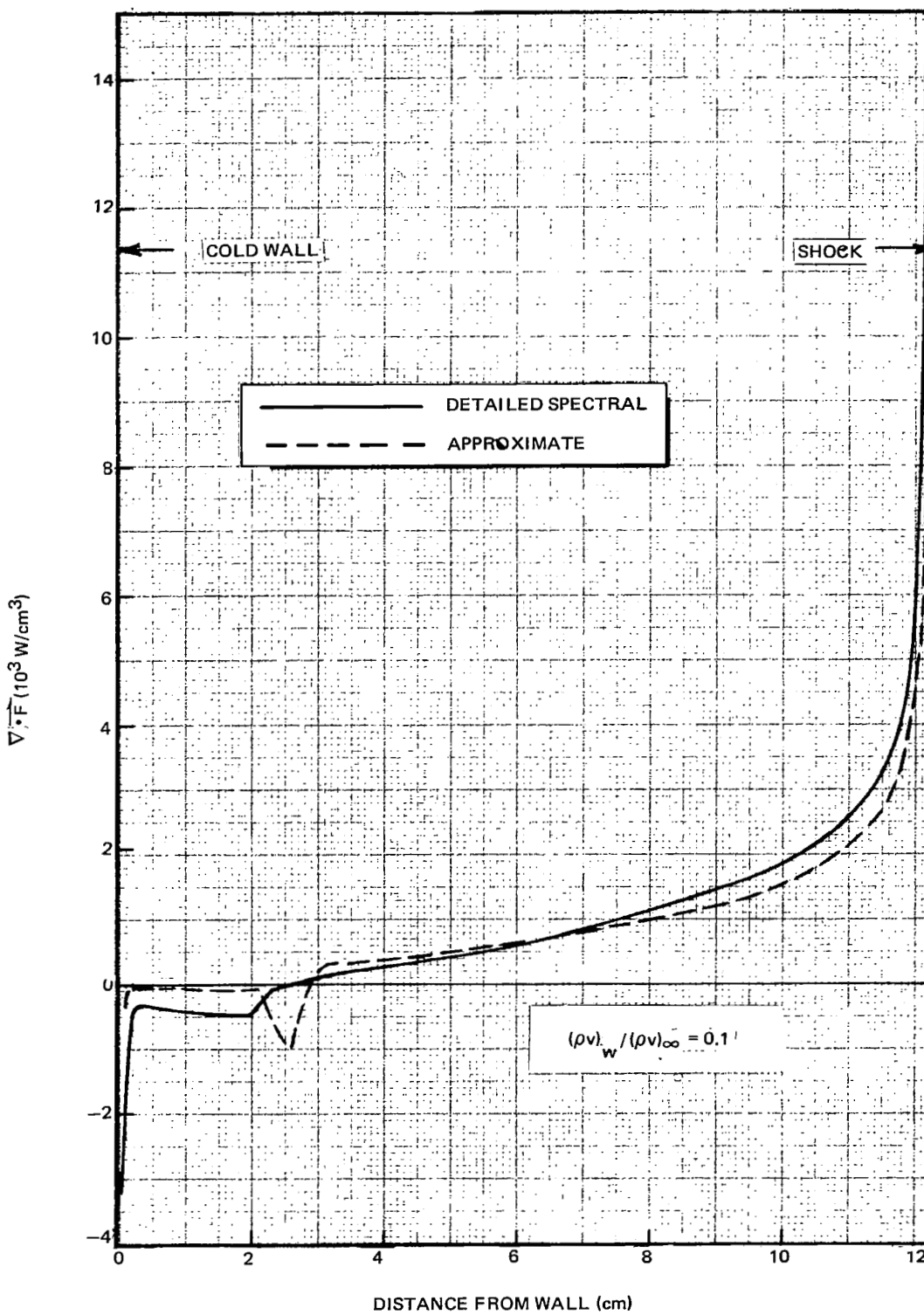


Figure 16. Divergence of Shock-Layer Radiation Compared to Approximation Using Continuum-Dominant Reabsorption $Bu_P^- = 0.000018$, $Bu_L = 0.0075$ (Case of Massive Blowing)

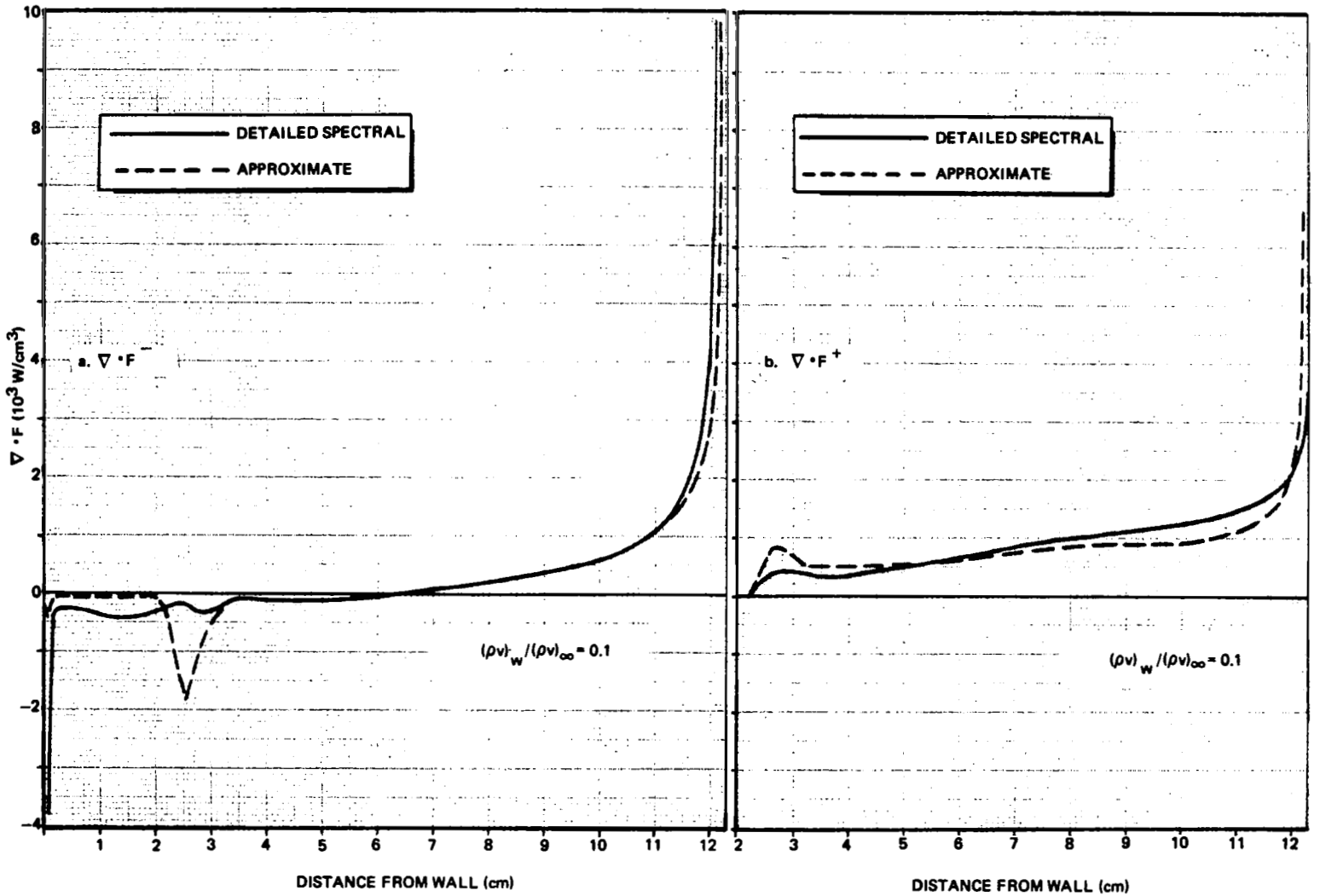


Figure 17. The Divergence of Shock-Layer Radiation Split into its Left-Moving and Right-Moving Components, Compared to Approximation using Continuum-Dominant Reabsorption Model $Bu_p = 0.000018$, $Bu_L = 0.0075$ (Case of Massive Blowing)

It is apparent that the radiation absorption mechanism in the blown-gas region is not that of an optically thick gas, for which $I_\omega \approx B^o_\omega$, but rather that of a pure absorbing gas, for which $I_\omega >> B^o_\omega$. The final step toward obtaining a good correlation in this region will be to replace the continuum reabsorption term, Equation (16), with the pure absorption term in Equation (18).

The approximate representation for $\nabla \cdot \vec{F}$ has been derived considering the important high-temperature radiative mechanisms leading to strong radiation-convection coupling. Under less severe entry conditions these mechanisms become less appropriate, but at the same time coupling is reduced and convection becomes dominant. Therefore, the use of the approximation for $\nabla \cdot \vec{F}$ at less severe entry conditions does not compromise the accuracy of the flow-field solutions. However, some loss in accuracy is expected for entry conditions more severe than those studied here.

Since the detailed spectral solutions revealed that a black wall has no effect on the radiative coupling, it was not necessary to develop a form for the approximate $\nabla \cdot \vec{F}$ to handle black walls. For the entry condition considered here almost half of the radiant energy incident on the wall is vacuum-ultraviolet, for which all materials are nearly black. Hence, the totally reflecting wall does not represent any real surface. At less severe entry conditions the fraction of vacuum-ultraviolet radiation incident on the wall can be less, but the radiative-convective coupling would then also be reduced. Therefore, the effect of wall reflectivity was neglected in the formulation of the approximate $\nabla \cdot \vec{F}$.

## CONCLUSIONS AND RECOMMENDATIONS

The stagnation-point shock-layer equations have been solved using detailed spectral calculation of the radiative-convective coupling. The solutions obtained are intended to provide verification for an approximate radiation-convection coupling calculation method. The results of the study have shown the following:

1. The originally proposed approximation for the divergence of the radiative flux is not suitable for accurate real-gas radiative-convective coupling calculations.
2. A new approximate formulation for $\nabla \cdot \vec{F}$ has been developed, such as to account for the important real-gas radiative transfer phenomena. The new approximate $\nabla \cdot \vec{F}$ adequately represents the $\nabla \cdot \vec{F}$ obtained from the detailed spectral calculations for the case of no mass injection. However, only fair agreement is observed for the case of massive blowing.
3. The modifications to the approximate relation for $\nabla \cdot \vec{F}$ necessary to provide good agreement with the detailed solutions with massive blowing have been identified.
4. For realistic entry bodies the radiative properties of the vehicle surface have a negligible effect on the radiative transfer in the shock layer.

On the basis of the results of this first phase of the study it is recommended that the effect of ambient-air radiative preheating be investigated early in the second phase of the study program. Appropriate inclusion of this effect can then be made in the subsequent calculations, if necessary. This effort in addition to the generation of solutions for the proposed no blowing cases will allow time to refine the continuum absorption term for the blowing cases. Also, it is recommended that additional detailed spectral solutions be generated. In particular, a detailed solution should be obtained for one of the proposed ablation-products-injection cases.

## Appendix A
## LINE TRANSFER IN OPTICALLY THICK MEDIA

In this appendix, an expression is derived for the divergence of the radiative flux from strong spectral lines. This expression involves two terms -- one "Planck-like" and one "Rosseland-like". The "Rosseland-like" term contains a "Rosseland-like" mean absorption coefficient, for which a simple expression is derived.

For strong lines, the intensity at y = 0 from an emitting-absorbing layer of thickness $\delta$ is given by Equation (10) of Reference 13 (Simmons), i.e.

$$I = (2\pi)^{1/2} \gamma_e \int_0^{\tau(\delta)} B^o_{\omega_i} (\tau') (\tau')^{-1/2} d\tau' \qquad (A-1)$$

where

$$\tau(y) = \frac{1}{2\pi \gamma_e} \int_0^y S(y') F(y') dy' \qquad (A-2)$$

$$k_\omega = \frac{S(T) F(T)}{\pi} \frac{\gamma_e}{\gamma_e^2 + (\omega_i - \omega)^2} \qquad (A-3)$$

$\omega_i$ = line center

S(T) F(T) = Simmons' terminology (Reference 13) for temperature dependent part of $k_\omega$

$\gamma_e$ = effective (constant) line half-width

$B^o_{\omega_i}$ = Planck function evaluated at line center

The intensity at some position $\tau(y)$ inside the layer is then seen to be

$$I = (2\pi)^{1/2}\ \gamma_e \int_0^{\tau} B^o_{\omega_i}(\tau')\ (\tau - \tau')^{-1/2}\ d\tau' \qquad (A-4)$$

where we have redefined y to be measured from the far boundary ($y_{new} = \delta - y_{old}$). Equation (A-4) is more suitable for our purpose than Equation (A-1); we now proceed to develop from Equation (A-4) an asymptotic form for $\nabla \cdot \vec{F}$.

Since the weighting of the black-body function is heaviest at $\tau' = \tau$, $B^o_\omega(\tau')$ can be approximated by

$$B^o_\omega(\tau') = B^o_\omega(\tau) + (\tau' - \tau)\frac{dB^o_\omega}{d\tau} + \ldots . \qquad (A-5)$$

or

$$I \approx (2\pi)^{1/2}\ \gamma_e \left[2B^o_{\omega_i}\ \tau^{1/2} - \frac{2}{3}\frac{dB^o_{\omega_i}}{d\tau}\ \tau^{3/2}\right] \qquad (A-6)$$

Thus the derivative of the intensity for a single line at $\omega_i$ is (neglecting terms with $\tau$ to powers greater than 1)

$$\frac{dI}{d\tau} = (2\pi)^{1/2}\ \gamma_e \left[\frac{dB^o_{\omega_i}}{d\tau}\ \tau^{1/2} + \frac{B^o_{\omega_i}}{\tau^{1/2}}\right] \qquad (A-7)$$

The first term represents the contribution from the optically thick region of the line and corresponds roughly to the Rosseland term of Equation (10). The second term, always positive, represents emission from the line wings and corresponds roughly to the Planck term of Equation (10), except that it has been derived for the case of optically thick line centers.

The following discussion develops a version of Equation (A-7) valid for complex line spectra by considering an appropriate average absorption coefficient.

Using an electron impact line-broadening model (Reference 8), the spectral absorption coefficient for the $i^{th}$ line is

$$k_{\omega,\ i} = N_i \frac{e^2}{m c g_o} (g_\ell\ f)_i \exp\left(-\frac{I_{\ell,\ i}}{kT}\right) \frac{b_i}{b_i^2 + (\omega - \omega_i)^2} \qquad \text{(A-8)}$$

where

$$b_i = \frac{N_e\ n_i^4}{A'\ (kT)^{1/2}\ (m+1)^2} \qquad \text{(A-9)}$$

Simmons' model for $k_\omega$ requires that the $b_i^2$ term in the denominator of Equation (A-8) be replaced by $\gamma_e^2$ -- the effective (constant) half width. It then follows, using Equations (A-3), (A-8), and (A-9) that

$$S_i(T)\ F_i(T) = \frac{\pi N_i\ N_e\ n_i^4\ (g_\ell\ f)_i\ e^2}{mcg_o\ A'\ \sqrt{kT}\ (m+1)^2\ \gamma_e} \exp\left(-\frac{I_{\ell,\ i}}{kT}\right) \qquad \text{(A-10)}$$

Define a group line strength, $\mathscr{S}$ such that

$$\frac{dB^o}{dT} \frac{1}{\gamma_e^{1/2}} \left[\int_0^y \mathscr{S}\, dy'\right]^{1/2} = \sum_i \frac{dB^o_{\omega_i}}{dT} \gamma_e^{1/2} \left[\int_0^y S_i\ F_i\ dy'\right]^{1/2} \qquad \text{(A-11)}$$

To find $\mathcal{IT}$ assume the following (used only for the derivation of $\mathcal{IT}$) in order to separate T- and i- dependent terms:

1. The most important lines originate in the ground state ($I_\ell = 0$).
2. Only one effective species contributes to the line radiation, of concentration N.

Then

$$S_i(T)\, F_i(T) = g(T)\, f_i \tag{A-12}$$

$$g(T) = \frac{\pi N(T)\, N_e(T)\, e^2}{m\, c\, g_o\, A'\, \sqrt{kT}\, (m+1)^2\, \gamma_e} \tag{A-13}$$

and

$$f_i = (g_\ell\, f)_i\, n_i^4 \tag{A-14}$$

Let

$$\frac{dB^o}{dT}\, \frac{1}{\gamma_e^{1/2}}\, \langle f \rangle^{1/2} = \gamma_e^{1/2} \sum_i \frac{dB^o_{\omega_i}}{dT}\, f_i^{1/2} \tag{A-15}$$

so that

$$\langle f \rangle^{1/2} = \frac{\gamma_e \sum_i \frac{dB^o_{\omega_i}}{dT}\, f_i^{1/2}}{\frac{dB^o}{dT}} \tag{A-16}$$

For a random distribution of lines and line strengths, $\langle f \rangle$ is independent of T, since the weighting function is then irrelevant. Thus for complex gas mixtures, we can have approximately for the first term in Equation (A-7)

$$\left(\frac{dI}{dy}\right)_l \approx \frac{dT}{dy}\frac{dB^o}{dT}\left[\frac{1}{\gamma_e}\int_0^y \langle f\rangle\, g(T)\, dy'\right]^{1/2} \tag{A-17}$$

$$= \frac{dT}{dy}\frac{dB^o}{dT}\left[\frac{1}{\gamma_e}\int_0^y \mathcal{J}\, dy'\right]^{1/2} \tag{A-18}$$

where

$$\left(\frac{\mathcal{J}}{\gamma_e}\right)^{1/2} = \sum_i \frac{dB^o_{\omega_i}}{dT}(\gamma_e S_i F_i)^{1/2} \Big/ \frac{dB^o}{dT} \tag{A-19}$$

and $\gamma_e S_i F_i$ is, from Equation (A-10), independent of the effective halfwidth, $\gamma_e$.

Define the "Rosseland-like" line absorption coefficient as

$$\bar{k}_L = \left[\sum_i \frac{dB^o_{\omega_i}}{dT}(\gamma_e S_i F_i)^{1/2} \Big/ \frac{dB^o}{dT}\right]^2 \tag{A-20}$$

and, assuming an infinite slab geometry, integration over solid angle gives finally

$$(\nabla \cdot \vec{F}^+)_l = \frac{4\pi}{3}\frac{dT}{dy}\frac{dB^o}{dT}\left[\int_0^y \bar{k}_L\, dy'\right]^{1/2} \tag{A-21}$$

Equation (A-21) is the expression for the "Rosseland-like" contribution to the divergence of the radiant energy flux of a line spectrum. It differs from the usual Rosseland approximation in that it depends upon the first derivative of the temperature rather than the second, and it depends upon the optical depth at which it is evaluated.

The first-order correction factor with which Equation (A-21) should be multiplied is obtained by retaining an additional term in Equation (A-5), and is given by (neglecting terms with $\tau$ to powers greater than 2)

$$\left[1 - \frac{1}{2}\frac{d \ln T}{dy}\tau - \frac{1}{6}\frac{d}{dy}\left(\ln \frac{dT}{dy}\right)\tau\right]$$

For the profile of Figure 2, in the region where Equation (A-21) is significant, the first correction is less than 0.1% of the value given by Equation (A-21).

A similar argument could be used to obtain an appropriate mean absorption coefficient for use in the second term of Equation (A-7). However, the temperature dependence of this mean $k_\omega$ is expected to be much the same as the usual Planck mean absorption coefficient. It is felt, therefore, that the derivation of a new mean absorption coefficient to be associated with the second term of Equation (A-7) ("Planck-like") is not warranted, but rather this term should be combined in some reasonable fashion with the usual Planck term; this procedure is illustrated in the main body of this report.

Therefore, integration of the second term of Equation (A-7) over solid angle and summing over all lines yields

$$(\nabla \cdot \vec{F}^+)_2 = 2\bar{k}'_P \frac{\sigma T^4}{\sqrt{\tau'_P}} \qquad \text{(A-22)}$$

where, in this case, the prime designates that these "Planck-like" mean values differ from the usual Planck mean, since they are averaged in a more complex fashion.

## Appendix B
## CONTINUUM TRANSFER IN OPTICALLY THICK MEDIA

In this appendix, an expression is derived for the divergence of the radiative flux from the uv continuum in optically thick media.

Assuming that the prime continuum contribution is in the vacuum UV, the Planck function reduces to Wien's radiation law

$$B^{o} \approx 2hc^{2}\omega^{3} \exp(-\theta\omega), \quad \theta = \frac{hc}{kT} \tag{B-1}$$

Assume a hydrogenic continuum dependence upon $\omega$, or

$$k_{\omega} \approx \frac{A(T)}{\omega^{3}} \quad \text{for } \omega \geq \omega_{c}$$

$$= 0 \quad \text{for } \omega < \omega_{c} \tag{B-2}$$

Let

$$\tau_{c} = \int_{0}^{y} A \, dy'$$

or $\tau_{c}$ is the reference optical depth evaluated at $\omega = 1 \text{ cm}^{-1}$.

The intensity is given by the integral solution to the Lambert-Bouguer law [Equation (7)]

$$I = \int_{0}^{\infty} \int_{0}^{y} B_{\omega}^{o}(y') \, k_{\omega}(y') \exp\left[-\int_{y'}^{y} k_{\omega}(y') \, dy''\right] dy' \, d\omega \tag{B-3}$$

or

$$I = 2hc^2 \int_{\omega_c}^{\infty} \exp\left(-\frac{\tau_c}{\omega^3}\right) \int_0^{\tau_c} \exp\left(-\theta\omega + \frac{\tau'_c}{\omega^3}\right) d\tau'_c \, d\omega \qquad \text{(B-4)}$$

or

$$\left(\frac{1}{2hc^2}\right)\frac{dI}{d\tau_c} = \int_{\omega_c}^{\infty} \exp\left(-\theta_{\tau_c}\omega\right) d\omega - \int_{\omega_c}^{\infty} \frac{\exp\left(-\frac{\tau_c}{\omega^3}\right)}{\omega^3} \int_0^{\tau_c} \exp\left(-\theta\omega + \frac{\tau'_c}{\omega^3}\right) d\tau'_c \, d\omega$$

(B-5)

Integrating by parts

$$\left(\frac{1}{2hc^2}\right)\frac{dI}{d\tau_c} = \int_{\omega_c}^{\infty} \exp\left(-\theta_o \omega - \frac{\tau_c}{\omega^3}\right) d\omega$$

$$- \int_0^{\tau_c} \frac{d\theta}{d\tau_c} \int_{\omega_c}^{\infty} \omega \exp\left(-\theta\omega - \frac{\tau_c}{\omega^3} + \frac{\tau'_c}{\omega^3}\right) d\omega \, d\tau'_c \qquad \text{(B-6)}$$

Only the second (absorption) term is important for our conditions, and it is important only for $\tau' \simeq \tau \gg 1$. Then

$$\frac{1}{2hc^2}\frac{dI}{d\tau_c} \approx -\frac{d\theta}{d\tau_c} \int_{\omega_c}^{\infty} \omega^4 \exp(-\theta\omega)\, d\omega \qquad \text{(B-7)}$$

which for large $\theta\omega_c$ can be approximated by

$$\frac{1}{2hc^2}\frac{dI}{d\tau_c} \approx -\frac{d\theta}{d\tau_c}\frac{1}{\theta^5}(\theta\omega_c + 1)^4 \exp(-\theta\omega_c) \qquad \text{(B-8)}$$

(The high-order terms of the 4th power binomial are correct.)

Integrating over solid angle gives

$$\left(\frac{dF^+}{dy}\right)_c = \frac{2\pi\, hc^2\, T^3}{(hc/k)^4} \frac{dT}{dy} \left(\frac{hc\,\omega_c}{kT} + 1\right)^4 \exp\left(-\frac{hc\,\omega_c}{kT}\right) \tag{B-9}$$

where this expression applies for large values of $\tau_c$.

Since the Stefan-Boltzmann constant is

$$\sigma = \frac{2k^4\,\pi^5}{15h^3\,c^2} \tag{B-10}$$

Equation (B-9) can be written

$$\left(\frac{dF^+}{dy}\right)_c = \frac{15}{\pi^4}\sigma T^3 \frac{dT}{dy} \left(\frac{hc\,\omega_c}{kT} + 1\right)^4 \exp\left(-\frac{hc\,\omega_c}{kT}\right) \tag{B-11}$$

## Appendix C

## AN APPROXIMATION TO THE FLUX DIVERGENCE FOR STRONG ABSORPTION

To treat the highly absorbed continua properly requires a model that allows radiative reabsorption without assuming an optically thick media. Thus the Lambert-Bouguer law becomes

$$\frac{dI_\omega}{ds} \approx -k_\omega I_\omega \text{ (strongly absorbing medium)} \tag{C-1}$$

instead of

$$\frac{dI_\omega}{ds} = k_\omega (B^o_\omega - I_\omega),\ B^o_\omega \approx I_\omega \text{ (optically thick media)} \tag{C-2}$$

To develop an approximate expression for $\nabla \cdot \vec{F}$, we average Equation (C-1) over solid angle and wave number using the following two assumptions: For the average over solid angle

$$I_\omega = \bar{I}_\omega \neq \text{function of } \cos\theta \tag{C-3}$$

For the average over wave number

$$F^+_\omega \propto B^o_\omega \tag{C-4}$$

Then

$$\frac{dF^+_\omega}{dy} = 2\pi \int_0^1 \frac{dI_\omega}{ds}\, d(\cos\theta) = -2\pi k_\omega \bar{I}_\omega \tag{C-5}$$

Also

$$F_\omega^+ = 2\pi \int_0^1 I_\omega \cos\theta \, d(\cos\theta) = \pi \bar{I}_\omega \tag{C-6}$$

or

$$\frac{dF_\omega^+}{dy} = -2k_\omega F_\omega^+ \tag{C-7}$$

Then

$$\frac{dF^+}{dy} = -2 \int_0^\infty k_\omega F_\omega^+ \, d\omega \tag{C-8}$$

or, using Equation (B-2)

$$\frac{dF^+}{dy} = -2 \int_{\omega_c}^\infty \frac{A}{\omega^3} F_\omega^+ \, d\omega \tag{C-9}$$

From Equation (C-4)

$$F_\omega^+ = KB_\omega^o \text{ (K is proportionality constant)} \tag{C-10}$$

$$\approx K \, 2hc^2 \omega^3 \exp\left(-\frac{hc\omega}{kT}\right) \text{ for large } \omega \tag{C-11}$$

Integrating Equation (C-10)

$$F^+ = K \frac{\sigma T^4}{\pi} \tag{C-12}$$

Integrating Equation (C-9) using Equation (C-11)

$$\frac{dF^+}{dy} = -4\,K\,AkTc\,\exp\left(-\frac{hc\omega_c}{kT}\right) \tag{C-13}$$

or, using Equation (C-12)

$$\frac{dF^+}{dy} = -\frac{4\pi kc}{\sigma T^3}\exp\left(-\frac{hc\omega_c}{kT}\right)AF^+ \tag{C-14}$$

Then, we can propose the following term to replace Equation (16):

$$\frac{dF^+}{dy} = -\frac{4\pi kc}{\sigma T^3}\exp\left(-\frac{hc\omega_c}{kT}\right)AF^+\left(\frac{\tau_c}{Bu_c + \tau_c}\right)^{1/2} \tag{C-15}$$

## REFERENCES


1. Howe, J. T.; and Viegas, J. R.: Solutions of the Ionized Radiating Shock Layer, Including Reabsorption and Foreign Species Effects, and Stagnation Region Heat Transfer, NASA TR R-159, 1963.

2. Hoshizaki, H.; and Wilson, K. H.: Convective and Radiative Heat Transfer During Superorbital Entry, AIAA J., vol. 5, 1967, pp. 25-35.

3. Anderson, J. D., Jr.: Non-gray Radiative Transfer Effects on the Radiating Stagnation Region Shock Layer and Stagnation Point Heat Transfer, NOLTR 67-104, 1967.

4. Chapman, G. T.: Heat Transfer in the Stagnation-Point Laminar Boundary Layer with Mass Transfer and Radiant Energy Absorption, Proceedings of the 1967 Heat Transfer and Fluid Mechanics Institute, Stanford University Press, 1967.

5. Dirling, R. B., Jr.; Rigdon, W. S.; and Thomas, M.: Stagnation-Point Heating Including Spectral Radiative Transfer, Proceedings of the 1967 Heat Transfer and Fluid Mechanics Institute, Stanford University Press, 1967.

6. Wiese, W. L.; Smith, M. W.; and Glennon, B. M.: Atomic Transition Probabilities, Vol. I, Hydrogen Through Neon: National Bureau of Standards, NSRDS - NBS 4, May, 1966.

7. Griem, H. R.: Plasma Spectroscopy, McGraw-Hill Book Co., New York, 1964.

8. Stewart, J. C.; and Pyatt, K. D., Jr.: Theoretical Study of Optical Properties - Photon Absorption Coefficients, Opacities, and Equations of State of Light Elements, Including the Effect of Lines, Report GA-2528, Vol. I (AFSWC-TR-61-71, Vol. 1), General Atomic Division, General Dynamics Corporation, September, 1961.

9. Penner, S. S.; and Thomas, M.: Approximate Theoretical Calculations of Continuum Opacities, AIAA J., Vol. 2, 1964, PP. 1672-1675.

10. Rigdon, W. S.; A Computer Code for Calculation of Transport Properties of High-Temperature Gases, Douglas Aircraft Company report DAC-59134 (in preparation).

11. Hoshizaki, H.; and Lasher, L. E.: Convective and Radiative Heat Transfer to an Ablating Body, AIAA Paper No. 67-327, presented at the AIAA Thermophysics Specialist Conference, New Orleans, Louisiana, April, 1967.

12. Thomas, M; and Rigdon, W. S.: A Simplified Formulation for Radiative Transfer. AIAA J., vol. 2, no. 11, November 1964, pp. 2052-2054.

13. Simmons, F. S.: Radiances and Equivalent Widths of Lorentz-Lines for Nonisothermal Paths. J. Quant. Spectrosc. Radiat. Transfer, vol. 7, no. 1, January/February 1967, pp. 111-121.



NASA-Langley, 1968 — 33 CR-1170